



Where might we find evidence of a Last Interglacial West Antarctic Ice Sheet collapse in Antarctic ice core records?

S.L. Bradley ^{a,*}, M. Siddall ^a, G.A. Milne ^b, V. Masson-Delmotte ^c, E. Wolff ^d

^a Department of Earth Sciences, University of Bristol, Bristol, UK

^b Department of Earth Sciences, University of Ottawa, Ottawa, Canada

^c Laboratoire des Sciences du Climat et de l'Environnement (IPSL/CEA-CNRS-UVSQ UMR 8212), Gif-sur-Yvette, France

^d British Antarctic Survey, Madingley Road, Cambridge, UK

ARTICLE INFO

Article history:

Received 30 November 2011

Accepted 17 March 2012

Available online 26 March 2012

Keywords:

isostasy

ice cores

Antarctic Ice Sheet

eustatic sea level

Last Interglacial

ABSTRACT

Abundant indirect evidence suggests that the West Antarctic Ice Sheet (WAIS) reduced in size during the Last Interglacial (LIG) compared to the Holocene. This study explores this possibility by comparing, for the first time, ice core stable isotope records for the LIG with output from a glacio-isostatic adjustment (GIA) model. The results show that ice core records from East Antarctica are remarkably insensitive to vertical movement of the solid land motion driven by a simulated hypothetical collapse of the WAIS. However, new and so far unexplored sites are identified which are sensitive to the isostatic signal associated with WAIS collapse and so ice core proxy data from these sites would be effective in testing this hypothesis further.

© 2012 Elsevier B.V. All rights reserved.

1. Introduction

The theories of climate-driven rapid ice sheet collapse and the instability of marine-based ice sheets were originally proposed over 30 years ago in the studies of Weertman (1976) and Mercer (1978). Despite numerous studies focusing on better understanding this response (Schoof, 2007; Gomez et al., 2010b; Katz and Worster, 2010), the instability of the West Antarctic Ice Sheet (WAIS) still remains a fundamental unknown for predicting future sea level rise. Evidence for the instability of the WAIS is found in the results from ice sheet modelling and paleoceanographic records which imply significant mass loss and possible rapid collapse events (Scherer et al., 1998; Bamber et al., 2009; Naish et al., 2009; Pollard and DeConto, 2009; Menviel et al., 2010; Teitler et al., 2010). However, major uncertainties and unknowns are still left unresolved regarding this past evolution (Huybrechts, 2009; Pollard and DeConto, 2009; Fyke et al., 2011; Huybrechts et al., 2011).

This study focuses on the evolution of the WAIS during the Last Interglacial (LIG), when global mean sea level is thought to have been significantly higher (4–9 m) than present (Kopp et al., 2009). As many studies have shown, this higher sea level cannot be explained due to only increased melting from valley glaciers and small ice caps (estimated -0.6 ± 0.1 m, Radić and Hock, 2010), ocean warming and thermal expansion (estimated -0.4 ± 0.3 m, McKay et al., 2011)

or increased mass loss from the Greenland Ice sheet (estimated between 0.4 and 4.4 m, Cuffey and Marshall, 2000; Otto-Bliesner et al., 2006; Robinson et al., 2011). This implies that a significant contribution (estimated from minimum of 3 m to over 6 m see, Bamber et al., 2009; Kopp et al., 2009) from the WAIS is required to fully produce the estimated sea levels during the LIG, motivating new study of the WAIS during the LIG.

Understanding the spatial and temporal history of the WAIS over the LIG is complicated due to sparse amount of direct evidence (i.e. geomorphological field observations such as periglacial trimlines or moraines). One recent study (Ackert et al., 2011) developed the first LIG elevation history for the WAIS across the Ohio Mountain Range by dating glacial erratics and ice-cored moraines. They concluded that the elevation of the ice sheet within this region did not change significantly during the LIG compared to present day (~ 125 m). Korotkikh et al. (2011) found evidence for LIG-age ice within the blue ice field Mount Mouton. Both these studies imply that during the LIG some ice remained across these regions of high ground but there still remains insufficient evidence to develop a complete spatial and temporal history of the ice sheet. Therefore one must rely upon indirect evidence to constrain the evolution of the WAIS over the LIG. Using such evidence is complicated because these data, unlike direct evidence, are sensitive not only to the impact of changes in the WAIS but also to multiple signals/processes within the climate system. Indirect records which have been adopted within previous studies have included: far-field sea level data which can be used to constrain changes in eustatic sea level (ESL) (Kopp et al., 2009); Paleoclimatic data (such as oceanic and ice core $\delta^{18}\text{O}$) combined with

* Corresponding author.

E-mail address: sarah.bradley@bristol.ac.uk (S.L. Bradley).

the results from climate/earth-system modelling to examine the response in surface temperature or ocean circulation following a WAIS collapse (due to the increase in the freshwater input) (Holden et al., 2010; Menviel et al., 2010; McKay et al., 2011); 3D numerical ice sheet models (Pollard and DeConto, 2009), which are forced by realistic climate and environmental records to recreate the spatial and temporal history of the Antarctic Ice Sheet (AIS) during a glacial–interglacial cycle.

Given the indirect evidence of past studies, many questions still remain unresolved, such as: did the WAIS fully collapse during the LIG, and if so, what caused this collapse? How rapid was it? What would be the impact on ESL and its contribution to global mean sea level? New approaches are needed to address these questions.

This study follows Siddall et al. (2012) by using a Glacial Isostatic Adjustment (GIA) model to investigate the sensitivity of ice core records to isostatically-driven changes in surface elevation resulting from changes in the ice thickness and movement of the solid land surface. Specifically, the impact of changes in surface elevation following a simulated collapse of the WAIS will be investigated using a series of stable isotope temperature proxies ($\delta^{18}\text{O}$ and δD) obtained from ice core records at six sites across the East Antarctic Ice Sheet (EAIS). This is the first time this approach has been taken to seek evidence for instability of the WAIS during the LIG.

A range of factors contribute to the observed isotope signal in ice core records, including changes in temperature, moisture origin and precipitation intermittency, site elevation (resulting from both changes in ice thickness and movement of the solid land surface; the latter dominated by GIA in most locations). Clearly, these factors complicate the task of isolating a possible vertical land motion signal. In this respect, the current study should be considered as a preliminary attempt at this goal. Our main purpose is to compute the isotopic signal due to GIA that would result from a collapse of the WAIS and make a first comparison to the observations without consideration of these other effects. Our motivation is to determine if such a signal would be resolvable in the ice core records and, if so, characterise its spatial pattern.

We first present a sensitivity study to investigate if isostatically-driven changes in surface elevation from a number of idealised models for the WAIS retreat will generate a resolvable δD signal at the EAIS core sites. Secondly, the spatial variation in this response will be described to provide information about the behaviour of the WAIS. Finally, ‘treasure maps’ will be generated which identify regions where future paleoclimatic data (such as ice core records) or geological/geomorphological field evidence will be sensitive to WAIS collapse through the associated changes in surface elevation and thus could provide useful information in constraining changes in the WAIS through the LIG. It is noted that the results presented within this manuscript should not be taken as an exact prediction, but rather as an indication of scale.

2. Data

2.1. Ice core data and caveats

Six ice core water stable isotope records, either $\delta^{18}\text{O}$ or δD , which cover the LIG were available for use within this paper. The location of these sites, source information, references and acronyms used in this paper are summarised in Fig. 1 and Table 1, with a more complete description of the data and inter-site variability given in Masson-Delmotte et al. (2011). All sites are located across the East Antarctic Plateau, with three sites (VK, DF and EDC) above 3000 m and three sites (TALDICE, TD and EDML) below 3000 m elevation. Although the database is limited to only 6 records, it provides a relatively even geographic spread across the EAIS, with EDML and DF located in NE region of the ice sheet, facing the Atlantic ocean; VK and EDC in the SE, facing the Indian ocean sector and TD and TALDICE on the

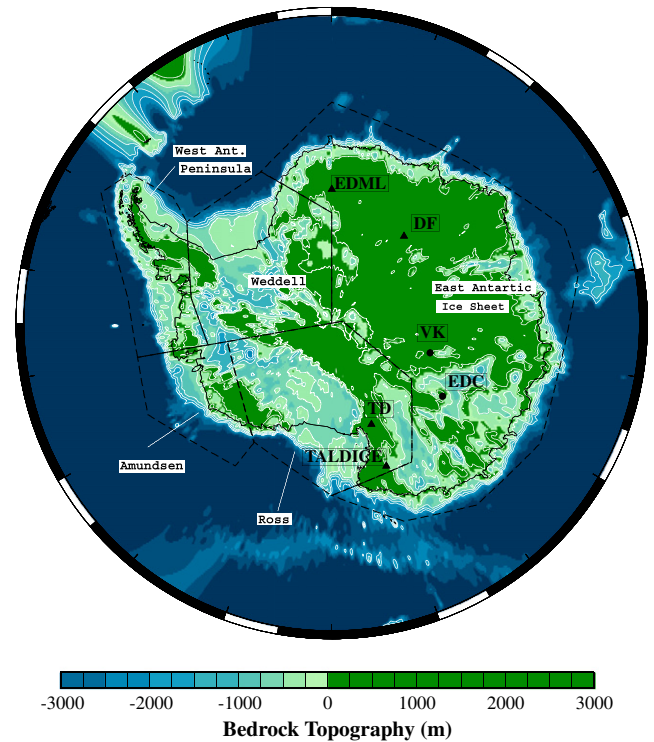


Fig. 1. Location map showing the six ice core sites discussed in this study (EPICA Dronning Maud Land (EDML), Dome Fuji (DF), Vostok (VK), EPICA Dome C (EDC), Taylor (TD) and Talos (TALDICE)). Also shown is the contoured bedrock topography (m) (Le Brocq et al., 2010b) to highlight the regions of the AIS which are located below present day sea level and the 5 different regions of the AIS which are referred to in this paper.

southern edge of the East Antarctic Plateau, facing the Ross Sea. At present there are no stable isotope records located across the WAIS which extend back to the LIG, although there is one recent LIG climatic record from a blue ice field located in Mount Moulton (Korotkikh et al., 2011) which can be used to infer the presence of LIG-age ice at this site.

Masson-Delmotte et al. (2011) describe in great detail the range of complicated factors which can contribute to the general spatial and temporal trends within the observed ice core, with some of the more important factors summarised below. As discussed within this publication, variations in the regional climate and the resultant variable response of the different sectors of the ice sheet are also important factors to consider when interpreting observed ice core records, especially when examining the higher resolution inter-site variability. As this study is interested in the gross characteristics of the six ice core records only, these higher resolution trends and regional climate variability are not explored within this study.

Local ice flow is one such influence on the ice core data. For example, records which are taken from ice ridges, such as EDML and VK, can be effected by advection, where the ice record is formed upstream and transported downstream to the final drill site location. An ‘upstream effect’ correction has been applied at EDML (Stenni et al., 2010) but not for VK where this effect was considered to be small over the period of interest (see discussion in Masson-Delmotte et al. (2011)). In comparison, records taken from ice domes, such as EDC, DF and TD are assumed to be located at the same geographic location as the drill site so that flow effects are considered to be minimal. Masson-Delmotte et al. (2011) noted that at TALDICE the flow pattern may be more complicated due to the possibility of flow from either side of the dome: either small glacier along the Transatlantic Mountains or into Wilkes Land and Ross Sea via ice streams. They concluded that over the LIG this affect would be small and so no correction was applied to these data.

Table 1

Summary details of the six Last Interglacial ice core data and associated references used within this paper, with locations marked in Fig. 1.

Site	Name	Symbol	Longitude	Latitude	Data	No. of points	Source
Taylor	TD	▲	158.717	−77.8	$\delta^{18}\text{O}$	13	Grootes et al. (2001)
TALOS	TALDICE	▲	159.1	−72.8	$\delta^{18}\text{O}$	39	Stenni et al. (2011)
VOSTOK	VK	●	106.8	−78.47	δD	309	Jouzel et al. (1993)
EPICA DOME C	EDC	●	123.38	−75.1	δD	424	Jouzel et al. (2007)
Dome Fuji	DF	▲	39.7	−77.317	$\delta^{18}\text{O}$	64	Watanabe et al. (2003)
Epica. Dron. Maud. Land	EDML	▲	0.067	−75	$\delta^{18}\text{O}$	176	EPICA members (2006)

In order to create a consistent framework for the comparison of each time series, all records will be considered in terms of units of δD equivalence. Therefore, the $\delta^{18}\text{O}$ records (see Table 1) were translated into δD using the global meteoric water line slope of 8. This may lead to errors associated with changes in air mass origins, affecting differently $\delta^{18}\text{O}$ and δD and reflected in deuterium excess. However, for ice cores where the two isotopes are available (EDC, EDML, VK and TD), this effect is marginal for the magnitude and trends during the Last Interglacial (Vimeux et al., 2001; Kawamura et al., 2007; Stenni et al., 2010; Masson-Delmotte et al., 2011).

Because the aim of this study is to examine the influence of changes in surface elevation at each ice core site, the predictions of surface elevation generated using the GIA model need to be converted into an equivalent change in δD . This requires an estimate of the relationship between changes in elevation and δD , which is known to be complicated, varying both spatially across an ice sheet due to changes in climate conditions (such as variations in the moisture source, topography of the ice sheet, and changes in temperature) (see Vinther et al., 2009; Masson-Delmotte et al., 2011). A recent study that examined Antarctica surface data calculated an average value of $-0.074\% \cdot \text{m}^{-1}$, decreasing to $-0.06\% \cdot \text{m}^{-1}$ for data from only the WAIS and increasing to $-0.08\% \cdot \text{m}^{-1}$ for all sites above 2000 m (e.g. Masson-Delmotte et al., 2008). As all the ice core sites are located at average present day elevations of >2000 m, an average value of $-0.08\% \cdot \text{m}^{-1}$ will be adopted for this study. It is noted that this value may have been both spatially and temporally variable during LIG, but currently there have been no studies which have studied this variability.

2.2. Age models and data interpretation

An issue to consider when comparing different ice core records is the dating method and age scale adopted. This is important in terms of the accuracy of the dating technique and the synchronisation of the differences in the timing of events between various paleoclimate records (i.e. marine, ice and terrestrial data) and of climate events between the Northern and Southern hemisphere (see Lemieux-Dudon et al. (2010) for a complete discussion). The latter is generally related to differences in the history of the Greenland Ice sheet and AIS. Within this paper the EDC3 age scale (Parrenin et al., 2007) was adopted for the six ice core records, to minimise uncertainties which arise due to differences in the absolute ages obtained between various age scales (which can be as high as 3 kyr) (Parrenin et al., 2007; Masson-Delmotte et al., 2010 supplementary information; Kawamura et al., 2007). A complete description of the methods used to transfer the EDC3 time scale to other cores and related issues are given in Masson-Delmotte et al. (2011).

All records used in this paper are referenced to a late-Holocene average (the mean over the last 3 kyr) taken from the initial data record (see list of sources in Table 1). Masson-Delmotte et al. (2011, see Fig. 4c) investigated a range of time intervals (0–1 kyr BP mean to a 0–3 kyr BP mean) to be used when defining a late Holocene reference value and found minimal difference in the final LIG ice core interpretations. The final δD record for each ice core site treated in this way is

shown in Fig. 2 between 138 and 118 kyr BP, a time interval which was taken to represent the transition from glacial conditions (~ 140 kyr BP) to the end of the interglacial, ~ 118 kyr BP for the LIG in Antarctica. It is noted that estimates for the LIG interval differ, with some sea level data suggesting an end closer to 115 kyr BP (Thomas et al., 2009, 2011).

Over the LIG, the 6 sites exhibit regional trends with both similarities and differences, with the gross characteristic of these records summarised below.

Following a sustained minimum, $\sim -40\%$ at 135 kyr BP, there is a steady rise in the δD record at all sites to reach a sustained peak (several kyrs) at 128 kyr BP. The rate of this rise appears to be consistent between most sites, although the magnitude of the peak in δD values is spatially variable, e.g. 40% at EDML, compared to 15% at TD. The timing of this rise was taken to indicate an average timing for the onset of the interglacial and retreat of the AIS (and will be used when constraining the ice models in Section 3). It is noted that this rise is not as well resolved at TD due to the limited number of data points. Following this peak, there is a rapid fall between 128 and 126 kyr BP, to reach a value close to present day values.

Towards the end of the LIG period, 126–118 kyr BP, there are some differences in the patterns of the δD records. At TALDICE there is a small rise in δD ($\sim 10\%$) sustained for 6 kyr, compared to a steady fall at DF ($\sim 20\%$) (a smaller fall was recorded at the other sites in the region). The variation in the records between these two sites compared to the other surrounding sites could be interpreted as indicating differences in either the local climate/temperature at these sites or the pattern of ice sheet history, either due to continued retreat (reduction elevation) at TALDICE or later sustained thickening (increasing in localised elevation) at DF.

A small secondary sharp fall, (120–118 kyr BP) highlighted by Masson-Delmotte et al. (2011) at the more coastal sites (EDML/TALDICE) will not be considered in this study but it was concluded that the cause of this was unlikely to be an abrupt increase in ice sheet elevation as the sites are located at significantly different locations across the AIS. Instead, these changes were attributed to a change in the distance to the open ocean, in relationship with sea ice extent, and variation in the regional high latitude moisture transport (although further investigation was recommended; Masson-Delmotte et al., 2011).

3. Method

3.1. Background and GIA model

At each ice core site, predictions of changes in surface elevation will be generated due to (a) changes in ice thickness only, (b) movement of the solid land surface only, (c) final surface elevation due to the relative change in distance between these two boundaries, i.e. combination of (a) and (b).

The ice thickness only changes in surface elevation will be calculated from the input ice model (see Section 3.2).

A GIA model is used to generate the predictions of surface elevation due to movement of the solid land surface, using the spectral technique described by Mitrovica et al. (1994) extended to incorporate the signal associated with GIA perturbations in Earth rotation.

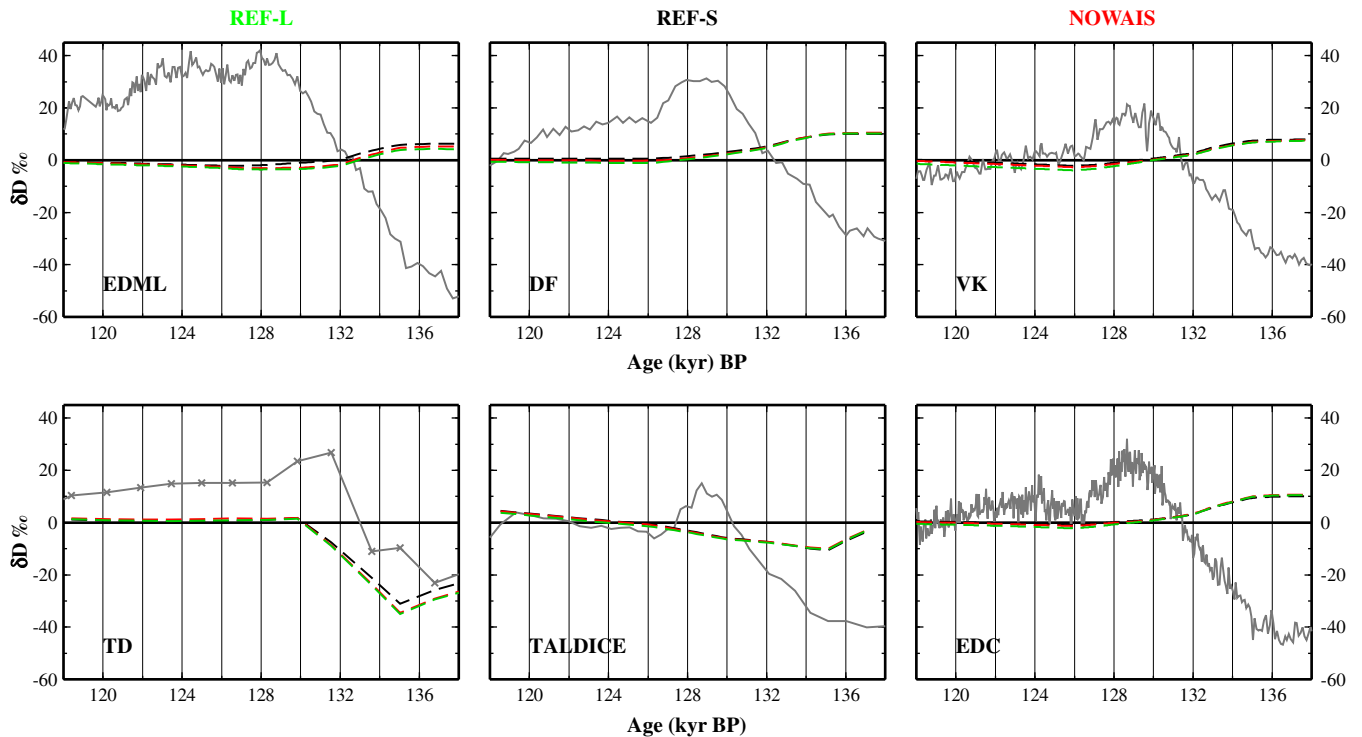


Fig. 2. Comparison of the observed δD (solid grey line) and predicted surface elevation-driven δD (dashed lines) due to both changes in ice thickness and movement of solid land surface, at the six ice core sites. Predictions of δD are shown for three LIG AIS models combined with the intermediate earth model (see main text); REF-L (green-dashed line), REF-S (black-dashed line) and NOWAIS (red-dashed line). Note that crosses are shown on the Taylor dome (TD) record to emphasise the lower resolution of this record. The TTLWAIS results plotted on top of the NOWAIS results and so are not shown. Given the similarity in the predicted δD signal from these three models, the differences in the predicted δD are shown in supplementary material (see Supplementary Fig. 2).

This model calculates the isostatic response of solid earth due to the mass redistribution resulting from both external (i.e. driven by ice-ocean mass redistribution due primarily to the growth and melting of ice sheets) and internal movement (solid earth). The input to the former is taken from the choice of input ice model (see Section 3.2).

Three user defined inputs are required to use the model: a model of Late Pleistocene ice history (see Section 3.2), an Earth model to reproduce the solid Earth deformation resulting from the surface mass redistribution (between the ice sheets and oceans) and a model of sea-level change to calculate the redistribution of ocean mass (e.g. Farrell and Clark, 1976).

The input Earth model is a spherically symmetric, self-gravitating Maxwell body, in which the elastic and density structure are taken from a seismic model (Dziewonski and Anderson, 1981), with a depth resolution of 10 km within the crust and 25 km in the mantle. The viscous structure is more crudely parameterised into three layers: a high viscosity (10^{43} Pa s) outer shell to simulate an elastic lithosphere, an upper mantle region of uniform viscosity extending from beneath the lithosphere to the 660 km seismic discontinuity and a lower mantle region of uniform viscosity extending from this depth to the core–mantle boundary. The lithosphere thickness and viscosity values within the upper and lower mantle are free parameters in the modelling.

The viscosity structure beneath the Antarctic continent is most likely characterised by significant lateral variability (Morelli and Danesi, 2004). Three earth models are considered which aim to encompass some of this variation: an intermediate model with a lithosphere thickness of 96 km, upper and lower mantle viscosities of 5×10^{20} Pa s and 1×10^{22} Pa s, respectively; a model to represent the region below the West Antarctic Archipelago, which is characterised by a relatively high heat flow and so a thinner lithosphere (71 km) and weaker upper mantle (1×10^{20} Pa s); and, finally, a model more typical for colder continental cratons such as that below the EAIS, with a thicker lithosphere (120 km) and greater upper mantle

viscosity (1×10^{21} Pa s). Note that the viscosity of the lower mantle is the same in each of the models considered. The parameters considered are broadly compatible with values inferred in previous GIA studies (e.g. Forte and Mitrovica, 1996; Davis et al., 1999; Kaufmann and Lambeck, 2002).

The input sea level model solves the generalised sea-level equation (Mitrovica and Milne, 2003; Kendall et al., 2005) and includes the most recent advances in GIA sea level modelling: time-varying shoreline migration, an accurate treatment of the sea level change in regions of ablating marine-based ice and the influence of GIA perturbations in the Earth's rotation vector (Milne and Mitrovica, 1998; Mitrovica et al., 2001, 2005).

Given that the observed δD value is defined relative to an 'average present day value' (see Section 2), it is important to ensure the same reference point is used when estimating the predicted surface elevation, prior to converting into an equivalent δD . To address this, all predictions were defined with respect to present day surface elevation. This is important for two key reasons: first to ensure a consistent reference point in time when comparing observed and predicted δD , and second to fully incorporate the effect of previous glaciations on the elevation changes over the LIG, where the system may not have returned fully to a state of equilibrium (as discussed in Lambeck et al. (2011)).

3.2. Ice models

Four models for the input ice history will be used to calculate changes in ice thickness at each ice core site and are described in greater detail below. Briefly, these are: (a) two reference Antarctic deglaciation models in which there is no WAIS collapse (i.e. the ice sheets retreat to a representative Holocene extent). The difference between these two models is the volume at the penultimate glacial maximum (PGM): the two values considered span the range of

plausible AIS ESL contributions (Section 3.2.2); (b) two follow-on models which simulate a collapse of the WAIS (in the more extreme of these two cases there is complete melting of this ice sheet; see Section 3.2.3).

3.2.1. Creation of a consistent time frame for T2 deglaciation

All ice models described within this study are adapted from a reference global ice model taken from Bassett et al., 2007 (which will be referred to as the Bassett et al. model in the following), which describes the evolution of all global ice sheets between 116 kyr and 0 kyr BP. This study combined the results of two earlier studies: (1) a glaciological AIS model (taken from Huybrechts, 2002) and (2) a global ice sheet model (Bassett et al., 2005) which was tuned to fit a suite of far-field relative sea level data from Last Glacial Maximum (LGM) to the present day. The Antarctic component of the final combined model, Bassett et al., was calibrated for the Holocene/Termination 1 (T1) using a suite of near field relative sea level data and field evidence taken from sites across Antarctica.

The AIS component of the Bassett et al. model was adapted to be more representative for T2 rather than T1, with all other global ice sheets (such as the Laurentide) unaltered. This approach follows a precedent for using T1 as a starting point for T2 as adopted in many previous studies (see Kopp et al., 2009; Lambeck et al., 2012). The revised timings and patterns for the deglaciation of the AIS (and associated periods of mass loss) during T2 will be constrained to those inferred from LIG AIS ice core and global far-field sea level records, and are summarised in the following stages.

- (1) In all models, prior to and at the PGM, defined as 140 kyr BP, it is assumed that all ice sheets have a similar glaciation phase and extent as during the most recent glacial cycle as in the Bassett et al. model.
- (2) For the reference AIS models (referred to as REF-L and REF-S in the following sections), the end of the LIG is defined as 118 kyr BP. At this time, it is assumed that the AIS reached a minimum extent similar to the present day extent (0 kyr BP) in the Bassett et al. model. This reference LIG extent will be adapted with the development of models of continued retreat across the WAIS (see Section 3.2.3).
- (3) The onset (135 kyr BP) and end (126 kyr BP) of deglaciation are taken to correlate with the onset of the rise in the AIS δD ice core records (see Fig. 2) and the 'average' timing for the global highstand during the LIG (i.e. Waelbroeck et al., 2008; Kopp et al., 2009) respectively. This created a deglaciation phase which extends over 11 kyr interval, that is separated into two main phases of mass loss: (i) between 135 and 128 kyr BP, where the AIS is assumed to have undergone the main period of mass loss which was taken to correlate peak change (hence warm period) in the AIS δD ice core records (see Fig. 2). (ii) smaller, but continued significant retreat between 128 and 126 kyr BP.
- (4) Finally, between 126 and 118 kyr BP, a continued thinning of ~100 m was imposed across the eastern edge of the Ross to try to capture the minor rise in the observed δD record (TALDICE) (see Section 2 and Fig. 2) with a predicted elevation-driven δD signal (see discussion in Masson-Delmotte et al. (2011)).

These provisional timings for the deglaciation will be applied to all AIS models presented and discussed in this paper. Although the models satisfy the primary observational constraints with respect to the timing of deglaciation and the LIG, there are very few constraints on AIS extent during the PGM and the chronology and pattern of retreat in different regions; as a result, these aspects of the models are not well constrained. In this respect, the small suite of ice models described here should be considered only as a subset of plausible scenarios to be used in this exploratory study.

3.2.2. Development of two reference models: a large or small AIS at the PGM?

As discussed above, there is a limited amount of quantitative evidence for the evolution of the AIS during T2, specifically which could be used to constrain the size of the AIS at the PGM and associated total ice volume loss during this deglaciation. Given this, the size of AIS during T1 was used as a guide when developing the PGM size of two reference models.

Even though there has been an extensive range of studies within the published literature into the evolution of the AIS during T1, the size of the AIS during this period and associated contribution to ESL has yet to be resolved. This is highlighted by the range of estimates within such studies (see Table 1, Bentley, 2010) from greater than 25 m (generally derived from glaciological or GIA modelling) to less than 5 m (derived from estimates using field evidence such as moraines, subglacial tills or erosional limits (trimlines)) (see Bentley, 1999).

Using this general picture of mass changes during T1 as a guide, and the provisional timings for deglaciation described in Section 3.2.1, two reference models were generated which consider two end-member sizes for the AIS at the PGM which will be referred to throughout this study as REF-L (large) and REF-S (small). The spatial extent at selected time steps and predicted ESL rise (defined relative to the Holocene) for these two models are illustrated in Figs. 3 and 4, respectively.

It is important to clarify the definition of ESL used when predicting the sea level rise as shown in Fig. 4 and discussed in this study. The term ESL assumes that all mass lost from land-based regions contributes directly to an increase in ocean volume. However, not all the mass lost from marine-based regions contributes directly to a change in ocean volume, as some of the sub-marine volume of melted ice is replaced by a mass of water. The calculation of 'effective ESL' (see Gomez et al., 2010b) takes this factor into account. Both these definitions for 'eustatic sea level' (ESL or effective ESL) are quoted within previous studies (see Jansen et al., 2007; Bamber et al., 2009; Gomez et al., 2010b) but do not represent the exact same estimate of ESL, as the effective ESL is always equal to, or less than the ESL value.

The REF-L model produces a ESL rise (as illustrated in Fig. 4) of ~23 m, with a ~20 m rise between 135 and 126 kyr BP (the main phase of AIS deglaciation). This is driven primarily by thinning and retreat within the Weddell (11 m) and Ross (7 m) Sea regions (compare Fig. 3a and c). This is more evident when examining the predicted ESL from these regions only (as shown on Supplementary Fig. 1 and Table 2). The total contribution of the EAIS component to ESL is relatively small (~+1 m), resulting from an early gradual thickening followed by a very minor thinning towards the end of the deglaciation. Between 126 and 118 kyr BP, the minor rise in the predicted ESL (~2.5 m) is due to combination of continued thinning across most regions of the AIS.

In comparison, the ESL rise from the REF-S model is ~7 m due to a thinner and more spatially restricted WAIS extent at the PGM (compare the ESL rise shown on Supplementary Fig. 1 and the values in Table 2). Note that the general timings of deglaciation are as described in Section 3.2.1 and the EAIS component and the minimum ice extent at 118 kyr BP remain unchanged from the REF-L model (see Fig. 3e).

3.2.3. Development of two WAIS collapse models: NOWAIS and TTLWAIS

As previously discussed, there are few published studies which have recreated the glacial–deglacial history of the WAIS during the LIG/T2 using a glaciological and/or climate driven ice model. Additionally, the lack of field evidence to constrain the spatial and vertical limits during this interval means that the nature of the retreat of the WAIS during a 'collapse event' has yet to be resolved. Therefore, to develop WAIS collapse models, a similar approach was adopted to other published studies (e.g. Bamber et al., 2009; Gomez et al.,

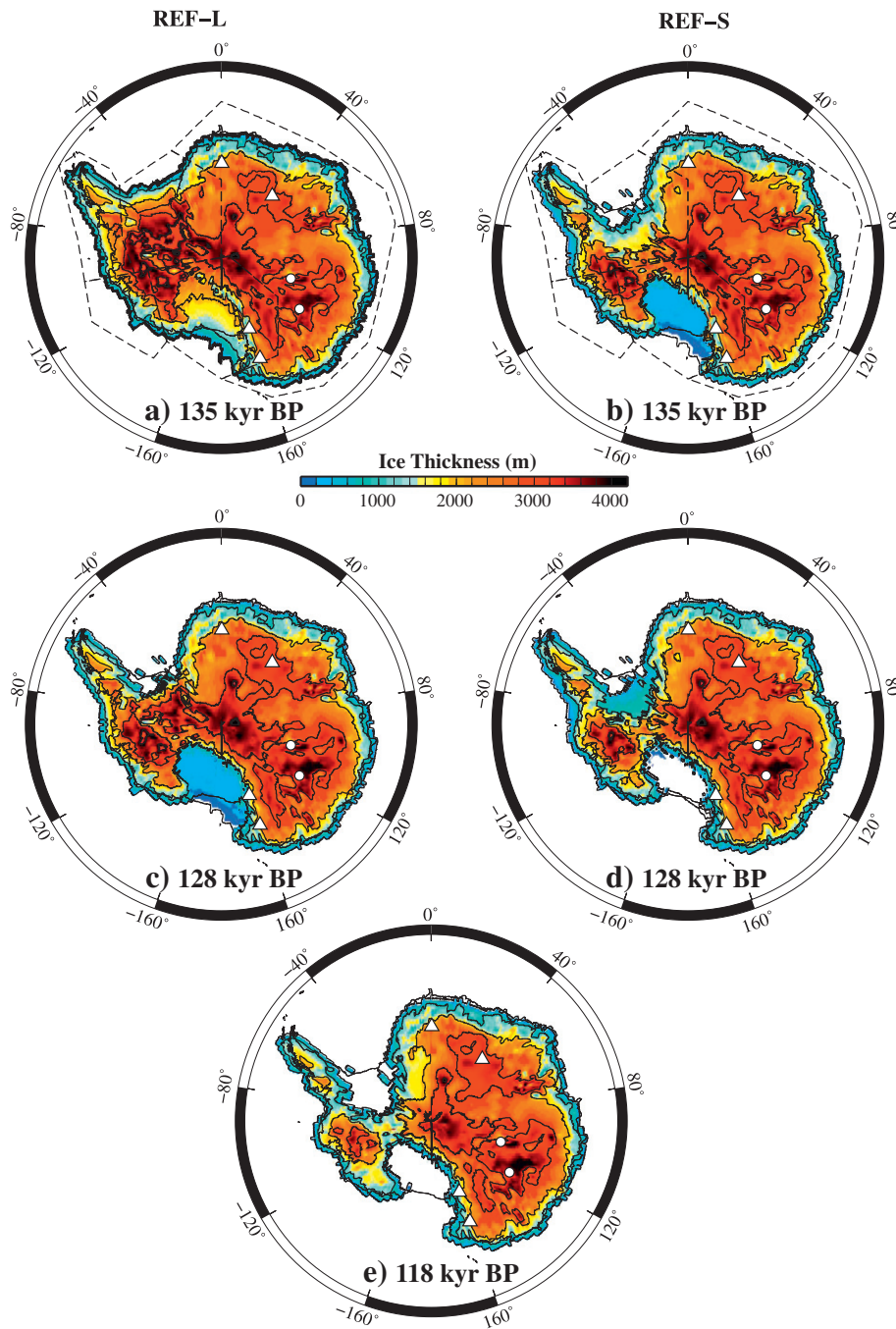


Fig. 3. Spatial plots of ice thickness at various time slices for the two reference AIS models at the following times (contour interval 1000 m): 135 kyr BP (a) REF-L and (b) REF-S; 128 kyr BP (c) REF-L and (d) REF-S. Both models retreat to the same final extent, as shown in (e) 118 kyr BP. On plots (a) and (b) the black lines mark the five regions shown in Fig. 1. The six ice core sites are shown in all plots.

2010b), which were based on the premise that the regions of the ice sheet which are marine-based, (i.e. grounded below present day sea level) could be susceptible to destabilisation and continued retreat. This theory is often referred to as 'marine-based ice sheet instability hypothesis', first proposed by Weertman (1976) and Mercer (1978) (see also Weertman, 1976; Vaughan and Spouge, 2002; Bamber et al., 2009). It is worth noting, however, that the specific processes controlling such a retreat are still not yet fully understood (see discussion in Bamber et al. (2009), Huybrechts (2009), and Pollard and DeConto (2009)).

To identify the spatial extent of such susceptible regions across the WAIS (the EAIS remains unchanged in our models), the most recent database of bedrock topography was used (Le Brocq et al., 2010a, as

contoured in Fig. 1). It is apparent from this map that loss of the marine-based sector would lead to significant ice loss within all four defined regions of the WAIS (Weddell, Ross, Amundsen Sea and West Antarctic Peninsula) with ice only remaining on the significantly elevated regions around the Marie-Byrd Land Ice cap (~110°W–140°W); regions of the West Antarctic Peninsula (~80°W–60°W) and the Ellsworth Mountains.

In the absence of more precise information, this mass loss was modelled as a continued retreat between 130 and 126 kyr BP (~4 kyr interval), to coincide with the approximate timing of the global LIG highstand adopted within this study (see above discussion including Stirling et al. (1998), Kopp et al. (2009), and Thomas et al. (2009)). There are few studies (see Table 1, Vaughan and Spouge

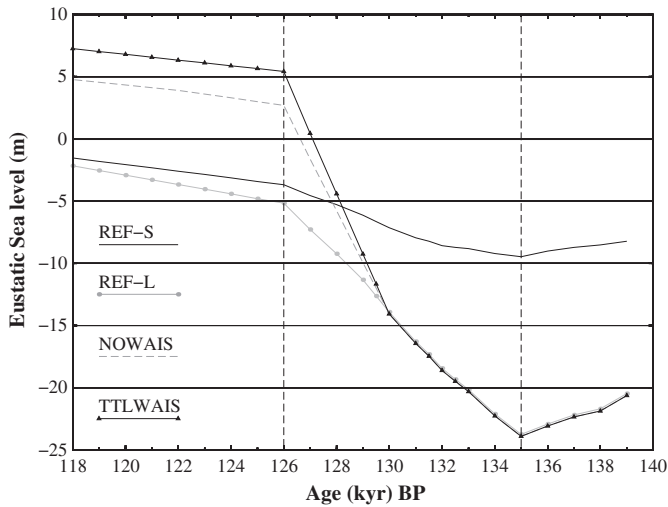


Fig. 4. Graph of the predicted eustatic sea level rise due to the AIS only calculated relative to present day (using the Bassett et al.) for the four ice models considered (see text for further information). Note that the two black dashed vertical lines mark the timing of the onset of deglaciation of the AIS (135 kyr BP) and the timing of the global highstand (126 kyr BP) as adopted in all four ice models.

(2002) and Pollard and DeConto (2009)) which examine the exact duration for such a collapse. Based on these, a 4 kyr interval was adopted as a reasonable starting estimate. This is supported by recent studies that show the stabilising effect of local RSL fall in regions of ice retreat (Gomez et al., 2010a).

Based on these criteria, the REF-L model was altered to create two WAIS collapse models: (a) NOWAIS (see Fig. 5c), where ice is lost in all regions defined as below present day sea level, leaving some ice on significantly elevated land areas. (b) TTLWAIS (see Fig. 5d), where ice is lost from all regions of the WAIS, grounded above or below present day sea level. This is an extreme collapse scenario, especially given the evidence for 'LIG-age' ice remaining across some regions of the WAIS (see Ackert et al., 2011; Korotkikh et al., 2011).

Table 2

Contributions to eustatic sea level from the AIS only from the four ice models discussed in this study (see text for details). (a) The contributions from each of the ice models for the total interglacial period (140–118 kyr BP) and between three selected time intervals: 140–135 kyr BP, prior to the onset of deglaciation; 135–126 kyr BP, the main phase of deglaciation of the AIS and 126–118 kyr, the final retreat phase. (b) Differences in the predicted eustatic sea level between the various LIG ice models over the interval 130–118 kyr BP (when the continued WAIS collapse is introduced): (a) REF-L and the NOWAIS, (b) REF-L and TTLWAIS and (c) the two WAIS collapse models: TTLWAIS and NOWAIS. The total contribution is also separated into the amount arising from the retreat within the four regions of the WAIS illustrated in Fig. 1: the Weddell, Ross, Amundsen and West Antarctic Peninsula.

a					
Time (kyr BP)	REF-S	REF-L	NOWAIS	TTLWAIS	
140–118	6.7	18.7	26.0	28.6	
140–135	–1.3	–3.4	–3.4	–3.4	
135–126	5.8	19.1	27.4	30.2	
126–118	2.2	3.0	2.1	1.8	
b					
130–118 (kyr BP)	All regions	Weddell	Ross	Amundsen	Peninsula
(a) 'REF-L' – NOWAIS	7.3	2.0	2.3	1.2	1.9
(b) 'REF-L' – TTLWAIS	9.8	2.6	3.1	1.4	2.8
(c) 'TTLWAIS' – 'NOWAIS'	2.6	0.6	0.8	0.3	0.9

However, it is used as an end-member scenario to investigate the maximum possible impact a WAIS retreat would generate across the EAIS ice core sites. Note that in both models the ice extent prior to and including 130 kyr BP is unchanged from the REF-L model and no revisions were made to the extent across the EAIS or along the elevated regions on the eastern edges of the Weddell and Ross Sea (Transatlantic Mountains). The final spatial extent within both models is similar to those proposed for such a retreat within other published studies, for example, for NOWAIS, Bamber et al., 2009 (their Fig. 2); Pollard and DeConto, 2009 (their Fig. 3b) and for REF_TTLWAIS, Bamber et al., 2009 (see their Fig. S3).

As is illustrated in Fig. 4 and summarised in Table 2, the increased mass loss within these two models would increase the ESL rise by ~7.5 m (NOWAIS) and 10 m (TTLWAIS). The minor rise between 126 and 118 kyr BP, is primarily sourced (as can be seen in Supplementary Fig. 1 and Table 2) from a small, continued thinning along the elevated regions on the eastern edge of the Weddell and Ross Sea and across selected regions of the EAIS. These estimates fall within a range of published values for the loss of the marine-based ice sheet from other studies, including Jansen et al. (2007) (5 m), Bamber et al. (2009) (4.8–3.7 m), and Gomez et al. (2010b) (8.4 m).

4. Modelling results and discussion

4.1. Results for the two LIG reference models (REF-L and REF-S)

Following the method outlined in Section 3 predictions of the surface elevation were generated at each ice core site for the REF-L and REF-S ice models, combined with the three earth viscosity models due to (a) changes in ice sheet thickness only; (b) movement of the solid land surface only; (c) final relative surface elevation change due to relative change in distance between these two boundaries (ice sheet thickness and land surface).

The predicted surface elevation change was converted into an equivalent δD (‰) (using the relationship described in Sections 2.1 and 3.1) and is compared to observed δD (‰) at each ice core site in Fig. 2. Because the difference in the predicted δD using the three earth models was minimal (for further discussion see Siddall et al., 2012), on average less than 1.4‰ at all sites, in Fig. 2 the results are shown only for the intermediate earth viscosity model.

There are a number of key points to conclude from the results shown in Fig. 2. First, it is possible to produce both a resolvable and significant elevation-driven δD signal at all the EAIS ice core sites due to changes in surface elevation using both the REF-L and REF-S models. This signal is driven predominately by elevation changes resulting from changes in the ice sheet thickness with a smaller contribution from movement in the solid land surface (as discussed in Siddall et al. (2012) and in Section 4.3).

Second, reducing the total size of the WAIS at the PGM (compare the results for REF-L to REF-S), has a very limited impact on the resultant δD signal (on average less than $\pm 2\%$, see Supplementary Fig. 2). This implies that the EAIS ice core sites are relatively insensitive to the maximum size of the WAIS at the PGM. This result also emphasises the limited spatial impact of the significant reduction in the total mass loss at the nearby ice core sites (i.e. EDML, TALDICE and TD).

Third, the sign (TD-TALDICE vs other sites) and variation in the magnitude of this predicted δD signal between the sites (10 to 40‰ compared to a total ~60‰ for the overall MIS6-MIS5 variation) can be used to indicate the spatial impact and sensitivity of the sites to detecting the elevation driven changes resulting from changes in the WAIS. Although the size of the predicted δD is much smaller at the four central EAIS sites (due to the relatively minor change in ice sheet thickness (deglacial thickening of ~100 m)), it highlights that even small changes in ice thickness will produce a resolvable predicted δD signal, if localised to the ice core site. This is again

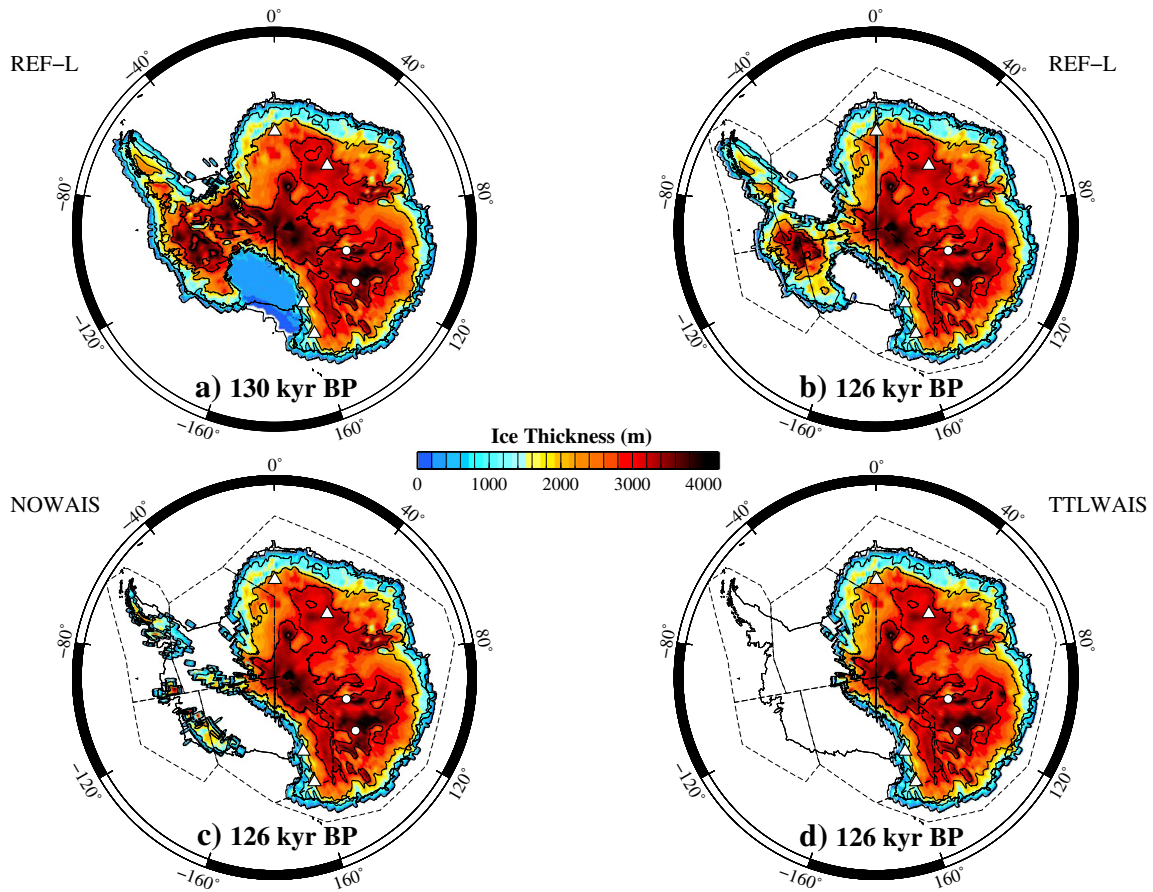


Fig. 5. Spatial plots of ice thickness to compare the WAIS collapse models to the REF-L model. The spatial extent of the REF-L is shown at 130 kyr BP (a) and 126 kyr BP (b); the two WAIS collapse models are shown at 126 kyr BP; (c) NOWAIS and (d) TTLWAIS. On all plots (b, c and d) the black lines mark the approximate location of the five regions shown in Fig. 1; locations of the six ice core sites are also shown. Note that continued retreat of the WAIS collapse models is introduced from 130 kyr BP, with the ice extent prior to this unchanged from REF-L.

highlighted by the minor rise in the predicted δD between 126 and 118 kyr BP at TALDICE which was generated by introducing minor thinning (fall in surface elevation) along the eastern edge of the Ross Sea over this period, which captures most of the observed δD trend.

To further emphasise the spatial component of these surface elevation-driven changes on the predicted δD , the predicted δD trend ($\%/\text{kyr}$) between 130 and 118 kyr BP for the REF-S and REF-L models was estimated and is illustrated in Fig. 6a and b, respectively. It is apparent that altering the size of the PGM WAIS would generate a significant signal across the central WAIS, ranging between $9\%/\text{kyr}$ and $20\%/\text{kyr}$ for the REF-S and REF-L models respectively. These results also highlight the predicted rise in the δD along the eastern edge of the Weddell and Ross Sea regions (as mentioned briefly above). Although the magnitude of this trend is smaller than that across the WAIS, $\sim 3\%/\text{kyr}$, given the relative size of the observed δD signal trend over this period (see Fig. 2), it is an important signal to consider when interpreting the observed trends in these ice core records. The factors controlling this spatial pattern will be evaluated in Section 4.3.

4.2. Investigating models of WAIS collapse over the LIG

The method outlined above was repeated for the two WAIS collapse models (NOWAIS and TTLWAIS) with the predicted δD generated at each of the six ice core sites (see Fig. 2) and spatial plots of the predicted δD trend ($\%/\text{kyr}$) between 130 and 118 kyr BP illustrated in Fig. 6(c and d). As the difference in the predicted δD at each ice core

site using these two models was minimal ($<0.4\%$), the results are shown only in Fig. 2 for the NOWAIS model only.

The main point to note comparing the three models in Fig. 2 is that large differences in the rate and timing of the ice loss across the WAIS do not generate a significant surface elevation signal across the EAIS resulting from either a change in ice thickness or movement of the solid land surface. The difference in the magnitude of the predicted δD signal is minimal, $<\pm 2\%$ (see Supplementary Fig. 2) compared to the REF-L model. The results imply that the present available range of EAIS ice core data would not be able to detect the GIA impact of a WAIS collapse during the LIG. In contrast, a significant surface elevation driven δD signal would be produced across most regions of the WAIS, which would generate an average rise of $>16\%/\text{kyr}$ (see Fig. 6c, d). If LIG ice core records were produced for this region, this signal can be used to aid in choosing optimal locations to detect past WAIS collapse events.

Preliminary investigations were conducted to evaluate the impact on these results of using smaller AIS (such as REF-S) for the background ice model in the development of the two WAIS collapse models. It was found that although the magnitude of predicted signal would be reduced, the spatial pattern and as such the maps shown in Fig. 6c and d remaining relatively unchanged. Therefore, these results were not included within the manuscript.

4.3. Understanding the impact of WAIS collapse across Antarctica

In this section, the origin and driving mechanisms behind the surface elevation changes produced in the simulations will be investigated

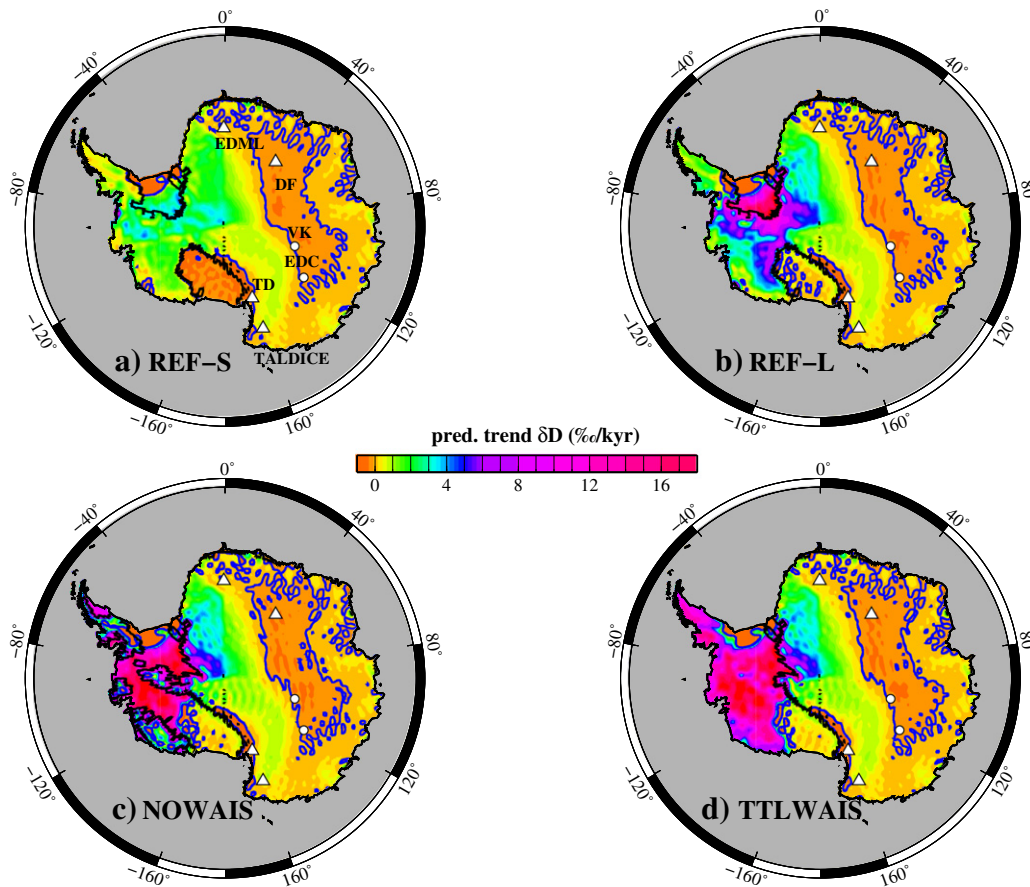


Fig. 6. Spatial plots of the elevation-driven (due to changes in ice thickness and movement of the solid land surface) predicted δD ($\%/kyr$) trend, averaged over 12 kyr interval defined between 130 and 118 kyr BP for the four LIG ice models: (a) REF-S, (b) REF-L, (c) NOWAIS and (d) TTLWAIS. On all plots the location of the 6 ice core sites is marked (see Table 1) with names highlighted on plot (a). The black line highlights the location of the edge of each ice model used. Note that dark red and orange colour represents $\%/kyr$ values greater than the maximum/minimum on the scale bar (20/–4), respectively, with the dark blue contour highlighting the 0 $\%/kyr$ trend.

by examining the spatial variation in surface elevation following WAIS collapse resulting from changes in ice thickness and movement of the solid land surface, the later which incorporates the isostatic-driven response of the solid earth. This will also address one of the main goals of this study: to identify regions which may be sensitive to detecting such a collapse (see Fig. 7).

Changes in surface elevation arise from the relative change in distance between two surfaces: (a) the ice sheet height over the glacial–interglacial cycles, (b) vertical movement of the solid land surface within the near-field are outlined in greater detail in a number of previous studies (Milne et al., 1999; Mitrovica et al., 2001; Kendall et al., 2005) and are primarily driven by the solid earth deformation associated with changes ice load and to a lesser extent changes in the ocean load. As an ice sheet deglaciates, this will typically produce an increase in the surface elevation across a central zone due to uplift associated with the reduction in the overlying ice load combined with lowering of the ice sheet height. This central region will typically be surrounded by a peripheral zone of decreasing land surface elevation due to the subsidence associated with the collapse of the forebulge. Although the impact of changes in the ocean load on the surface elevation is smaller than those associated with the ice load, a significant amount of solid earth deformation is still generated and will be particularly important within marine-based regions of the ice sheet.

To highlight the impact of the continued WAIS collapse in terms of such variations, spatial plots of the difference in the predicted surface elevation between the REF-L and NOWAIS models at 126 kyr BP are shown in Fig. 7 for (a) changes in ice thickness only, (b) changes in the height of

the solid land surface only, due to ice–ocean loading and rotational effects (results are shown so that positive values indicate an increase in land height and vice-versa), (c) the total surface elevation change, which is the combination of the results in (a) and (b). It is noted that if these results were repeated for the REF-S, to consider the impact of a smaller PGM model, there would be minimal impact on the spatial patterns shown in Fig. 7. The main difference, as can be seen comparing Fig. 6a and b, would be a reduction in the total amplitude of the signal.

Examining the results in Fig. 7, it is apparent that the changes in ice thickness dominate the total surface elevation changes. Despite this, there is still a resolvable, although significantly smaller response in the height of the solid land surface (Fig. 7b), where the land height increases by more than 500 m. This response is highly concentrated over regions of the WAIS (between Ellsworth Mountains (north) and Marie Byrd Land to the south), and generally reflects the geometry of ice thinning (Fig. 7a). Across the EAIS where the ice core sites are located, the signal is much smaller, with a less than 10 m (Fig. 7b) fall in the land height.

These results support those shown in Figs. 2 and 6 that the simulated WAIS collapse does not generate a significant surface elevation signal across in East Antarctica due to the movement of the solid land surface, which as discussed in Section 3.1, incorporates the isostatic response of the solid earth due to mass redistribution. This is due to the relatively limited spatial extent of the mass loss in a WAIS collapse scenario and also the replacement of marine-based ice by ocean water (which acts to dampen the isostatic response) (Milne et al., 1999; Gomez et al., 2010b).

Finally, the spatial plot of the difference in predicted surface elevation (between the REF-L and NOWAIS models) (Fig. 7c) can be used

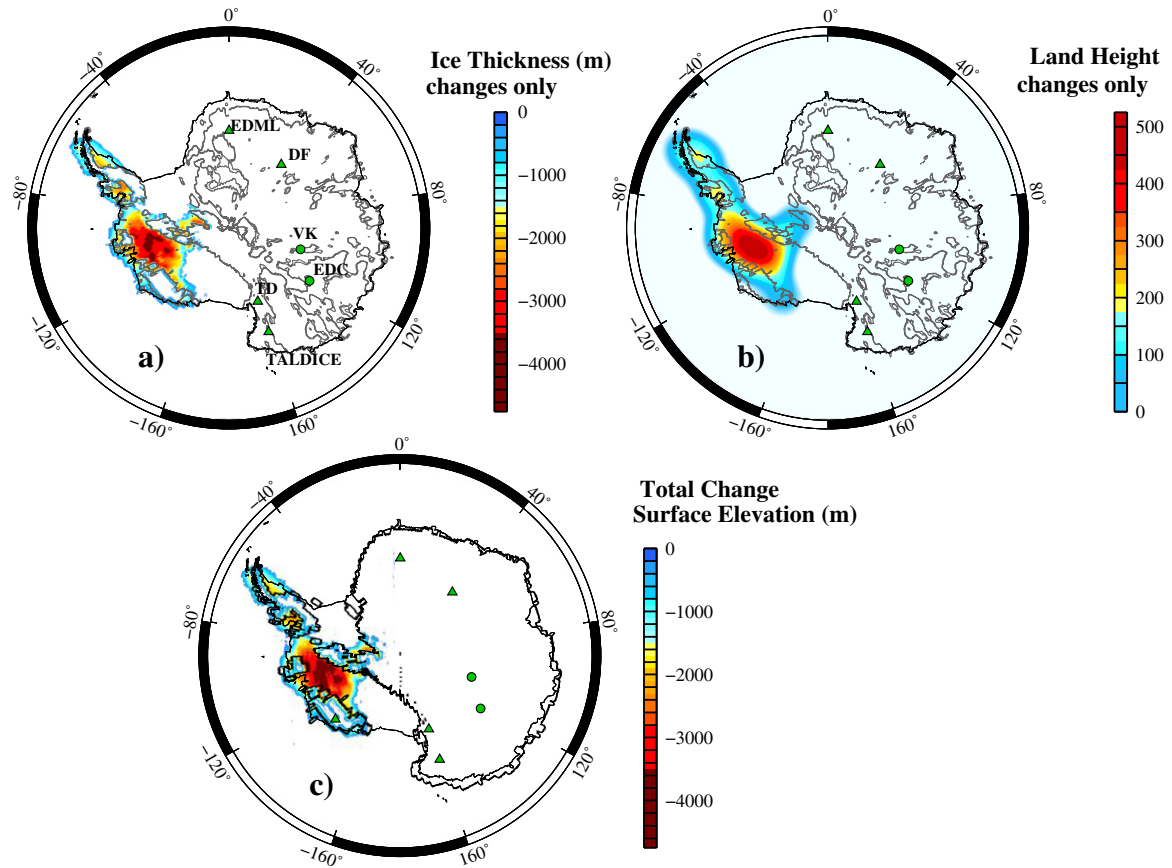


Fig. 7. Spatial plots of the difference in the total predicted surface elevation using the REF-L and NOWAIS icemodels at 126 kyr BP due to: (a) changes in ice thickness only, (b) changes in the elevation of the solid land surface due to ice-ocean loading and rotational effects (c) total change in surface elevation due to the combination of (a) and (b). Additionally, on each plot is shown the location of the six ice core sites (with names shown on (a)) and the contoured bedrock topography (m) (Le Brocq et al., 2010b), to highlight the regions of the AIS which are located below present day sea level. Note that the black circle and triangle marked on (c) show the location of two sites where LIG-age ice has been detected and discussed in text: black circle from Ohio Mountain Range (see Ackert et al., 2011) and the black triangle from the Mt. Moulton Blue Ice area (see Korotkikh et al., 2011).

to identify regions which would have good sensitivity to a WAIS collapse. These include the West Antarctic Peninsula or within the central WAIS (where an open seaway would develop following a collapse).

Following such a simulated collapse, it is noted that LIG-age ice may still remain within these higher ground regions or in small valley glaciers, such as evident in the previously discussed studies of Ackert et al. (2011) and Korotkikh et al. (2011).

The two maps shown in Figs. 6c and 7c can be used as resource by the wider scientific community to identify regions which would be sensitive to detecting this collapse and used to constrain the behaviour of the WAIS during T2. The results shown in Fig. 7c would be more appropriate as a guide within geological studies which using techniques such as exposure age dating or mapping of geomorphological landforms, provide information on the change in the surface elevation of the ice sheet (i.e. Ackert et al., 2011).

In contrast, the spatial plot of the predicted trend in δD ($\%/kyr$) (Fig. 6c) would be a more suitable guide to identify sites within studies which produce paleoclimate records (such as ice-core reconstructions). Evidence from either of these types of studies would be useful to delimit the spatial extent of the WAIS and rule out the more extreme collapse model investigated in this paper (TTLWAIS).

5. Conclusions

This study has examined the influence of isostatically-driven changes in surface elevation on the predicted LIG δD at six ice core sites from across the EAIS for four AIS models. Two of these models were developed to examine the impact of changes in the size of the

AIS at the PGM and the remaining two were developed to examine the impact of a continued deglaciation to include a WAIS collapse.

Our results show that the changes in the evolution of the WAIS within these four AIS models do not generate a significant elevation-driven δD signal at the six ice core sites. That is, the isostatic response to changes in the WAIS over the LIG is not large across the EAIS and so δD from EAIS ice cores cannot be used to assess WAIS stability over this period. As the results in Figs. 6 and 7 illustrate, the spatial response to WAIS collapse is concentrated in regions of the WAIS which have undergone significant changes in ice thickness.

The maps shown in Figs. 6c and 7c could be used by the wider community/field scientists as a 'treasure map' for identifying sites where results from geological studies (such as exposure ages) and/or new paleoclimate data (such as ice-core reconstructions), would be sensitive to the impact of a WAIS collapse on the surface elevation and therefore suitable for constraining the evolution of the WAIS during the LIG.

Supplementary materials related to this article can be found online at doi:10.1016/j.gloplacha.2012.03.004.

Acknowledgements

Mark Siddall is supported by an RCUK fellowship and the University of Bristol. This is a contribution to the PALSEA working group. This is Past4Future contribution no. 12. The research leading to these results has received funding from the European Union's Seventh Framework Programme (FP7/2007-2013) under grant agreement no. 243908, "Past4Future. Climate change - Learning from the past climate". Glenn

Milne acknowledges support from the Natural Sciences and Engineering Research Council of Canada and the Canada Research Chairs program. Eric Wolff is supported by the British Antarctic Survey's Polar Science for Planet Earth programme, funded by NERC. Valerie Masson-Delmotte acknowledges support by the ANR DOME A project (ANR-07-BLAN-0125). The Talos Dome Ice core Project (TALDICE), a joint European programme, is funded by national contributions from Italy, France, Germany, Switzerland and the United Kingdom. Primary logistical support was provided by PNRA at Talos Dome. This is TALDICE publication no is 19.

References

- Ackert Jr., R.P., Mukhopadhyay, S., Pollard, D., DeConto, R.M., Putnam, A.E., Borns Jr., H.W., 2011. West Antarctic Ice Sheet elevations in the Ohio Range: geologic constraints and ice sheet modeling prior to the last highstand. *Earth and Planetary Science Letters* 307 (1–2), 83–93.
- Bamber, J.L., Riva, R.E.M., Vermeersen, B.L.A., LeBrocq, A.M., 2009. Reassessment of the potential sea-level rise from a collapse of the West Antarctic Ice Sheet. *Science* 324 (5929), 901–903.
- Bassett, S.E., Milne, G.A., Mitrovica, J.X., Clark, P.U., 2005. Ice sheet and solid earth influences on far-field sea-level histories. *Science* 309 (5736), 925–928.
- Bassett, S.E., Milne, G.A., Bentley, M.J., Huybrechts, P., 2007. Modelling Antarctic sea-level data to explore the possibility of a dominant Antarctic contribution to meltwater pulse 1A. *Quaternary Science Reviews*, 26 (17–18), 2113–2127.
- Bentley, M.J., 1999. Volume of Antarctic Ice at the Last Glacial Maximum, and its impact on global sea level change. *Quaternary Science Reviews* 18 (14), 1569–1595.
- Bentley, M.J., 2010. The Antarctic palaeo record and its role in improving predictions of future Antarctic Ice Sheet change. *Journal of Quaternary Science* 25 (1), 5–18.
- Cuffey, K.M., Marshall, S.J., 2000. Substantial contribution to sea-level rise during the last interglacial from the Greenland ice sheet. *Nature* 404 (6778), 591–594.
- Davis, J.L., Mitrovica, J.X., Scherneck, H.G., Fan, R., 1999. Investigations of Fennoscandian glacial isostatic adjustment using modern sea level records. *Journal of Geophysical Research, Solid Earth* 104 (B2), 2733–2747.
- Dziwonski, A.M., Anderson, D.L., 1981. Preliminary reference earth model. *Physics of the Earth and Planetary Interiors* 25 (4), 297–356.
- EPICA Members, 2006. One-to-one coupling of glacial climate variability in Greenland and Antarctica. *Nature*, 444 (7116), 195–198.
- Farrell, W.E., Clark, J.A., 1976. Postglacial sea-level. *Geophysical Journal of the Royal Astronomical Society* 46 (3), 647–667.
- Forte, A.M., Mitrovica, J.X., 1996. New inferences of mantle viscosity from joint inversion of long-wavelength mantle convection and post-glacial rebound data. *Geophysical Research Letters* 23 (10), 1147–1150.
- Fyke, J.G., Weaver, A.J., Pollard, D., Eby, M., Carter, L., Mackintosh, A., 2011. A new coupled ice sheet/climate model: description and sensitivity to model physics under Eemian, Last Glacial Maximum, late Holocene and modern climate conditions. *Geoscientific Model Development* 4 (1), 117–136.
- Gomez, N., Mitrovica, J.X., Huybers, P., Clark, P.U., 2010a. Sea level as a stabilizing factor for marine-ice-sheet grounding lines. *Nature Geoscience* 3 (12), 850–853.
- Gomez, N., Mitrovica, J.X., Tamisieu, M.E., Clark, P.U., 2010b. A new projection of sea level change in response to collapse of marine sectors of the Antarctic Ice Sheet. *Geophysical Journal International* 180 (2), 623–634.
- Groote, P.M., Steig, E.J., Stuiver, M., Waddington, E.D., Morse, D.L., 2001. The Taylor dome antarctic O-18 record and globally synchronous changes in climate. *Quaternary Research* 56 (3), 289–298.
- Holden, P.B., Edwards, N.R., Wolff, E.W., Lang, N.J., Singarayer, J.S., Valdes, P.J., Stocker, T.F., 2010. Interhemispheric coupling, the West Antarctic Ice Sheet and warm Antarctic interglacials. *Climate of the Past* 6 (4), 431–443.
- Huybrechts, P., 2002. Sea-level changes at the LGM from ice-dynamic reconstructions of the Greenland and Antarctic ice sheets during the glacial cycles. *Quaternary Science Reviews* 21 (1–3), 203–231.
- Huybrechts, P., 2009. Global change West-side story of Antarctic ice. *Nature* 458 (7236), 295–296.
- Huybrechts, P., Goelzer, H., Janssens, I., Driesschaert, E., Fichefet, T., Gooze, H., Loutre, M.F., 2011. Response of the Greenland and Antarctic Ice Sheets to multi-millennial greenhouse warming in the earth system model of intermediate complexity LOVE-CLIM. *Surveys in Geophysics* 32 (4–5), 397–416.
- Jansen, E., Overpeck, J., Briffa, K.R., Duplessy, J.-C., Joos, F., Masson-Delmotte, V., Olago, D., Otto-Bliesner, B., Peltier, W.R., Rahmstorf, S., Ramesh, R., Raynaud, D., Rind, D., Solomina, O., Villalba, R., Zhang, D., 2007. Paleoclimate. In: Solomon, S. (Ed.), *Climate Change 2007: the physical science basis. Contribution of Working Group I to the Fourth Assessment Report of the Intergovernmental Panel on Climate Change*. Cambridge University Press, pp. 433–497.
- Jouzel, J., Barkov, N.I., Barnola, J.M., Bender, M., Chappellaz, J., Genthon, C., Kotlyakov, V.M., Lipenkov, V., Lorius, C., Petit, J.R., Raynaud, D., Raisbeck, G., Ritz, C., Sowers, T., Stievenard, M., Yiou, F., Yiou, P., 1993. Extending the Vostok Ice-Core Record of the Paleoclimate to the Penultimate Glacial Period. *Nature*, 364 (6436), 407–412.
- Jouzel, J., Masson-Delmotte, V., Cattani, O., Dreyfus, G., Falourd, S., Hoffmann, G., Minster, B., Nouet, J., Barnola, J.M., Chappellaz, J., Fischer, H., Gallet, J.C., Johnsen, S., Leuenberger, M., Loulergue, L., Luethi, D., Oerter, H., Parrenin, F., Raisbeck, G., Raynaud, D., Schilt, A., Schwander, J., Selmo, E., Souchez, R., Spahni, R., Stauffer, B., Steffensen, J.P., Stenni, B., Stocker, T.F., Tison, J.L., Werner, M., Wolff, E.W., 2007. Orbital and millennial Antarctic climate variability over the past 800,000 years. *Science*, 317 (5839), 793–796.
- Katz, R.F., Worster, M.G., 2010. Stability of ice-sheet grounding lines. *Proceedings of the Royal Society A: Mathematical, Physical and Engineering Science* 466 (2118), 1597–1620.
- Kaufmann, G., Lambeck, K., 2002. Glacial isostatic adjustment and the radial viscosity profile from inverse modeling. *Journal of Geophysical Research, Solid Earth* 107 (B11), 15.
- Kawamura, K., Parrenin, F., Lisiecki, L., Uemura, R., Vimeux, F., Severinghaus, J.P., Hutterli, M.A., Nakazawa, T., Aoki, S., Jouzel, J., Raymo, M.E., Matsumoto, K., Nakata, H., Motoyama, H., Fujita, S., Goto-Azuma, K., Fujii, Y., Watanabe, O., 2007. Northern Hemisphere forcing of climatic cycles in Antarctica over the past 360,000 years. *Nature* 448 (7156), 912–914.
- Kendall, R.A., Mitrovica, J.X., Milne, G.A., 2005. On post-glacial sea level – II. numerical formulation and comparative results on spherically symmetric models. *Geophysical Journal International* 161 (3), 679–706.
- Kopp, R.E., Simons, F.J., Mitrovica, J.X., Maloof, A.C., Oppenheimer, M., 2009. Probabilistic assessment of sea level during the last interglacial stage. *Nature*, 462 (7275), 863–867.
- Korotkikh, E.V., Mayewski, P.A., Handley, M.J., Sneed, S.B., Introne, D.S., Kurbatov, A.V., Dunbar, N.W., McIntosh, W.C., 2011. The last interglacial as represented in the glaciochemical record from Mount Moulton Blue Ice Area, West Antarctica. *Quaternary Science Reviews* 30 (15–16), 1940–1947.
- Lambeck, K., Purcell, A., Dutton, A., 2012. The anatomy of interglacial sea levels: the relationship between sea levels and ice volumes during the Last Interglacial. *Earth and Planetary Science Letters* 315–316, 4–11.
- Le Brocq, A.M., Payne, A.J., Vieli, A., 2010a. An improved Antarctic dataset for high resolution numerical ice sheet models (ALBMAP v1). *Earth System Science Data Discussions* 3 (1), 247–260.
- Le Brocq, A.M., Payne, A.J., Vieli, A., 2010b. An improved Antarctic dataset for high resolution numerical ice sheet models (ALBMAP v1). *Earth System Science Data Discussions* 3 (1), 195–230.
- Lemieux-Dudon, B., Blayo, E., Petit, J.R., Waelbroeck, C., Svensson, A., Ritz, C., Barnola, J.M., Narcisi, B.M., Parrenin, F., 2010. Consistent dating for Antarctic and Greenland ice cores. *Quaternary Science Reviews* 29 (1–2), 8–20.
- Masson-Delmotte, V., Hou, S., Ekaykin, A., Jouzel, J., Aristarain, A., Bernardo, R.T., Bromwich, D., Cattani, O., Delmotte, M., Falourd, S., Frezzotti, M., Gallee, H., Genoni, L., Isaksson, E., Landais, A., Helsen, M.M., Hoffmann, G., Lopez, J., Morgan, V., Motoyama, H., Noone, D., Oerter, H., Petit, J.R., Royer, A., Uemura, R., Schmidt, G.A., Schlosser, E., Simoes, J.C., Steig, E.J., Stenni, B., Stievenard, M., van den Broeke, M.R., de Wal, R., de Berg, W.J.V., Vimeux, F., White, J.W.C., 2008. A review of Antarctic surface snow isotopic composition: observations, atmospheric circulation, and isotopic modeling. *Journal of Climate* 21 (13), 3359–3387.
- Masson-Delmotte, V., Stenni, B., Blunier, T., Cattani, O., Chappellaz, J., Cheng, H., Dreyfus, G., Edwards, R.L., Falourd, S., Govin, A., Kawamura, K., Johnsen, S.J., Jouzel, J., Landais, A., Lemieux-Dudon, B., Lourantou, A., Marshall, G., Minster, B., Mudelsee, M., Pol, K., Rothlisberger, R., Selmo, E., Waelbroeck, C., 2010. Abrupt change of Antarctic moisture origin at the end of Termination II. *Proceedings of the National Academy of Sciences of the United States of America* 107 (27), 12091–12094.
- Masson-Delmotte, V., Buiron, D., Ekaykin, A., Frezzotti, M., Gallee, H., Jouzel, J., Krinner, G., Landais, A., Motoyama, H., Oerter, H., Pol, K., Pollard, D., Ritz, C., Schlosser, E., Sime, L.C., Sodemann, H., Stenni, B., Uemura, R., Vimeux, F., 2011. A comparison of the present and last interglacial periods in six Antarctic ice cores. *Climate of the Past* 7 (2), 397–423.
- McKay, N.P., Overpeck, J.T., Otto-Bliesner, B.L., 2011. The role of ocean thermal expansion in Last Interglacial sea level rise. *Geophysical Research Letters* 38, 6.
- Menviel, L., Timmermann, A., Timm, O.E., Mouchet, A., 2010. Climate and biogeochemical response to a rapid melting of the West Antarctic Ice Sheet during interglacials and implications for future climate. *Paleoceanography* 25, 12.
- Mercer, J.H., 1978. West Antarctic Ice Sheet and CO₂ greenhouse effect – threat of disaster. *Nature* 271 (5643), 321–325.
- Milne, G.A., Mitrovica, J.X., 1998. Postglacial sea-level change on a rotating Earth. *Geophysical Journal International* 133 (1), 1–19.
- Milne, G.A., Mitrovica, J.X., Davis, J.L., 1999. Near-field hydro-isostasy: the implementation of a revised sea-level equation. *Geophysical Journal International* 139 (2), 464–482.
- Mitrovica, J.X., Milne, G.A., 2003. On post-glacial sea level: I. general theory. *Geophysical Journal International* 154 (2), 253–267.
- Mitrovica, J.X., Davis, J.L., Shapiro I.I., 1994. A SPECTRAL FORMALISM FOR COMPUTING 3-DIMENSIONAL DEFORMATIONS DUE TO SURFACE LOADS .1. THEORY. *Journal of Geophysical Research-Solid Earth*, 99 (B4), 7057–7073.
- Mitrovica, J.X., Milne, G.A., Davis, J.L., 2001. Glacial isostatic adjustment on a rotating earth. *Geophysical Journal International* 147 (3), 562–578.
- Mitrovica, J.X., Wahr, J., Matsuyama, I., Paulson, A., 2005. The rotational stability of an ice-age earth. *Geophysical Journal International* 161 (2), 491–506.
- Morelli, A., Danesi, S., 2004. Seismological imaging of the Antarctic continental lithosphere: a review. *Global and Planetary Change* 42 (1–4), 155–165.
- Naish, T., Powell, R., Levy, R., Wilson, G., Scherer, R., Talarico, F., Krissek, L., Niessen, F., Pompilio, M., Wilson, T., Carter, L., DeConto, R., Huybers, P., McKay, R., Pollard, D., Ross, J., Winter, D., Barrett, P., Browne, G., Cody, R., Cowan, E., Crampton, J., Dunbar, G., Dunbar, N., Florindo, F., Gebhardt, C., Graham, I., Hannah, M., Hansaraj, D., Harwood, D., Helling, D., Henrys, S., Hinnov, L., Kuhn, G., Kyle, P., Lauffer, A., Maffioli, P., Magens, D., Mandernack, K., McIntosh, W., Millan, C., Morin, R., Ohneiser, C., Paulsen, T., Persico, D., Raine, I., Reed, J., Riesselman, C., Sagnotti, L., Schmitt, D., Sjunneskog, C., Strong, P., Taviani, M., Vogel, S., Wilch, T.,

- Williams, T., 2009. Obliquity-paced Pliocene West Antarctic ice sheet oscillations. *Nature*, 458 (7236), 322–328.
- Otto-Bliesner, B.L., Marsha, S.J., Overpeck, J.T., Miller, G.H., Hu, A.X., 2006. Simulating arctic climate warmth and icefield retreat in the last interglaciation. *Science* 311 (5768), 1751–1753.
- Parrenin, F., Barnola, J.M., Beer, J., Blunier, T., Castellano, E., Chappellaz, J., Dreyfus, G., Fischer, H., Fujita, S., Jouzel, J., Kawamura, K., Lemieux-Dudon, B., Loulergue, L., Masson-Delmotte, V., Narcisi, B., Petit, J.R., Raisbeck, G., Raynaud, D., Ruth, U., Schwander, J., Severi, M., Spahni, R., Steffensen, J.P., Svensson, A., Udisti, R., Waelbroeck, C., Wolff, E., 2007. The EDC3 chronology for the EPICA dome C ice core. *Climate of the Past* 3 (3), 485–497.
- Pollard, D., DeConto, R.M., 2009. Modelling West Antarctic ice sheet growth and collapse through the past five million years. *Nature* 458 (7236), 329–332.
- Radić, V., Hock, R., 2010. Regional and global volumes of glaciers derived from statistical upscaling of glacier inventory data. *J. Geophys. Res.* 115, F01010. doi:10.1029/2009JF001373.
- Robinson, A., Calov, R., Ganopolski, A., 2011. Greenland ice sheet model parameters constrained using simulations of the Eemian Interglacial. *Climate of the Past* 7 (2), 381–396.
- Scherer, R.P., Aldahan, A., Tulaczyk, S., Possnert, G., Engelhardt, H., Kamb, B., 1998. Pleistocene collapse of the West Antarctic ice sheet. *Science* 281 (5373), 82–85.
- Schoof, C., 2007. Ice sheet grounding line dynamics: steady states, stability, and hysteresis. *Journal of Geophysical Research* 112 (F3), F03S28.
- Siddall, M., Milne, G.A., Masson-Delmotte, V., 2012. Uncertainties in elevation changes and their impact on Antarctic temperature records since the end of the last glacial period. *Earth and Planetary Science Letters*, 315–316, 12–23.
- Stenni, B., Masson-Delmotte, V., Selmo, E., Oerter, H., Meyer, H., Röthlisberger, R., Jouzel, J., Cattani, O., Falourd, S., Fischer, H., Hoffmann, G., Iacumin, P., Johnsen, S.J., Minster, B., Udisti, R., 2010. The deuterium excess records of EPICA Dome C and Dronning Maud Land ice cores (East Antarctica). *Quaternary Science Reviews* 29 (1–2), 146–159.
- Stenni, B., Buiron, D., Frezzotti, M., Albani, S., Barbante, C., Bard, E., Barnola, J.M., Baroni, M., Baumgartner, M., Bonazza, M., Capron, E., Castellano, E., Chappellaz, J., Delmonte, B., Falourd, S., Genoni, L., Iacumin, P., Jouzel, J., Kipfstuhl, S., Landais, A., Lemieux-Dudon, B., Maggi, V., Masson-Delmotte, V., Mazzola, C., Minster, B., Montagnat, M., Mulvaney, R., Narcisi, B., Oerter, H., Parrenin, F., Petit, J.R., Ritz, C., Scarchilli, C., Schilt, A., Schupbach, S., Schwander, J., Selmo, E., Severi, M., Stocker, T.F., Udisti, R., 2011. Expression of the bipolar see-saw in Antarctic climate records during the last deglaciation. *Nature Geoscience*, 4 (1), 46–49.
- Stirling, C.H., Esat, T.M., Lambeck, K., McCulloch, M.T., 1998. Timing and duration of the Last Interglacial: evidence for a restricted interval of widespread coral reef growth. *Earth and Planetary Science Letters* 160 (3–4), 745–762.
- Teitler, L., Warnke, D.A., Venz, K.A., Hodell, D.A., Becquey, S., Gersonde, R., Teitler, W., 2010. Determination of Antarctic Ice Sheet stability over the last ~500 ka through a study of iceberg-rafted debris. *Paleoceanography* 25 (1), PA1202.
- Thomas, A.L., Henderson, G.M., Deschamps, P., Yokoyama, Y., Mason, A.J., Bard, E., Hamelin, B., Durand, N., Camoin, G., 2009. Penultimate deglacial sea-level timing from uranium/thorium dating of Tahitian corals. *Science* 324 (5931), 1186–1189.
- Thompson, W.G., Allen Curran, H., Wilson, M.A., White, B., 2011. Sea-level oscillations during the last interglacial highstand recorded by Bahamas corals. *Nature Geoscience* 4 (10), 684–687.
- Vaughan, D.G., Spouge, J.R., 2002. Risk estimation of collapse of the West Antarctic Ice Sheet. *Climatic Change* 52 (1), 65–91.
- Vimeux, F., Masson, V., Delaygue, G., Jouzel, J., Petit, J.R., Stievenard, M., 2001. A 420,000 year deuterium excess record from East Antarctica: information on past changes in the origin of precipitation at Vostok. *Journal of Geophysical Research-Atmospheres* 106 (D23), 31863–31873.
- Vinther, B.M., Buchardt, S.L., Clausen, H.B., Dahl-Jensen, D., Johnsen, S.J., Fisher, D.A., Koerner, R.M., Raynaud, D., Lipenkov, V., Andersen, K.K., Blunier, T., Rasmussen, S.O., Steffensen, J.P., Svensson, A.M., 2009. Holocene thinning of the Greenland ice sheet. *Nature* 461 (7262), 385–388.
- Waelbroeck, C., Frank, N., Jouzel, J., Parrenin, F., Masson-Delmotte, V., Genty, D., 2008. Transferring radiometric dating of the last interglacial sea level high stand to marine and ice core records. *Earth and Planetary Science Letters* 265 (1–2), 183–194.
- Watanabe, O., Jouzel, J., Johnsen, S., Parrenin, F., Shoji, H., and Yoshida, N., 2003. Homogeneous climate variability across East Antarctica over the past three glacial cycles. *Nature* 422 (6931), 509–512.
- Weertman, J., 1976. Glaciologists grand unsolved problem. *Nature* 260 (5549), 284–286.